Int. J. Heat Mass Transfer. Vol. 31, No. 1, pp. 55–65, 1988
Printed in Great Britain

0017-9310/88 $3.00 + 0.00

CHF enhancement in flowing fluorocarbon liquid films using structured surfaces and flow deflectors

T. A. GRIMLEY,† I. MUDAWWAR and F. P. INCROPERA
Boiling and Two-phase Flow Laboratory, School of Mechanical Engineering, Purdue University, West Lafayette, IN 47907, U.S.A.

(*Received* 11 *February* 1987 *and in final form* 5 *June* 1987)

Abstract—Boiling experiments were performed with a fluorocarbon (FC-72) liquid film falling over a vertical heated surface. Severe boiling separated most of the film from the surface, leaving a thin subfilm, and CHF was associated with dryout of the subfilm. Surfaces with microfin augmentation enhanced CHF with respect to smooth or microstud surfaces. A louvered plate mounted parallel to the heated surface also increased CHF by deflecting the separated liquid back to the heated surface and delaying subfilm dryout.

INTRODUCTION

BOILING in liquid films provides an efficient heat transfer process for applications such as thin film evaporators and the cooling of turbine blades and electronic components. In the case of electronic cooling, however, a major drawback relates to the low heat fluxes associated with dielectric fluorocarbons, which are considered to be best suited for direct contact with electronic components. The maximum heat flux which may be dissipated is limited by the critical heat flux (CHF), which defines the upper limit of the efficient range of boiling heat transfer.

Several investigators have studied boiling and CHF in thin films [1–4] and have reported that the onset of CHF corresponds to film breakdown for which a large portion of the film separates from the heated surface, leaving a thin subfilm in contact with the surface. At CHF the subfilm begins to dry out near the trailing edge of the heater, and the unwetted region extends upstream towards the film inlet. Katto and Ishii [2] studied CHF in a film directed along rectangular surfaces which were 10, 15 and 20 mm long and 15 mm wide. For film velocities in the range from 1.5 to 15 m s^{-1} and film thicknesses of 0.56 and 0.77 mm, CHF was correlated for R-113 and water by the expression

$$\frac{q_M}{\rho_g h_{fg} U} = 0.0164 \left[\frac{\rho_f}{\rho_g}\right]^{0.867} \left[\frac{\sigma}{\rho_f U^2 L}\right]^{0.333}. \quad (1)$$

In electronic cooling applications involving boiling, FC-72 is typically chosen as the working fluid, since its boiling point at atmospheric pressure ($\sim$56°C) is substantially less than the maximum allowable temperature for electronic components ($\sim$85°C). From equation (1) a film of FC-72 at atmospheric pressure, flowing with a velocity of $U = 1$ m s^{-1} over a 50 mm long heated surface, would have a critical heat flux of $q_M = 5.5$ W cm^{-2}.

Augmentation of the surface geometry offers one method of improving heat transfer performance and extending CHF. The basic principles used to enhance pool boiling also apply to boiling in liquid films. Early studies of pool boiling enhancement focused on the use of roughened surfaces, which provided short-term improvements in the nucleate boiling regime but had little effect on CHF. The roughened surfaces became ineffective when the relatively large surface cavities were flooded with liquid and could no longer serve as artificial nucleation sites. However, long-term improvement in the nucleate boiling regime can be provided by surfaces having a large density of re-entrant cavities which tend to trap vapor embryos and therefore maintain active nucleation sites [5]. Examples of commercially available surfaces include those having porous sintered coatings (Union Carbide, HIGH-FLUX), re-entrant grooves (Wieland-erke AG, GEWA-T), and surfaces formed by bending notched fins to form porous cover plates with subsurface tunnels (Hitachi, THERMOEXCEL-E). Pool boiling tests conducted by Bergles and Chyu [6] and Marto and Lepere [7] showed that the temperature overshoot (hysteresis) associated with the inception of boiling in fluorocarbon liquids was more pronounced for the foregoing surfaces than for smooth surfaces.

Most studies of boiling with augmented surfaces have been restricted to the nucleate boiling regime. However, Marto and Lepere [7] reported FC-72 CHF data for pool boiling from the THERMOEXCEL-E, HIGH-FLUX and GEWA-T surfaces. Although CHF values for the THERMOEXCEL-E and HIGH-FLUX surfaces differed little from those obtained for a smooth surface, the GEWA-T surface was operated in stable nucleate boiling at a heat flux which was 17%

† Current address: Fluid and Thermal Systems Group, Southwest Research Institute, San Antonio, TX 78284, U.S.A.

NOMENCLATURE

C	constant
c_p	specific heat
$\bar{e}$	average absolute percent error
$\bar{e}_{max}$	maximum percent error
h_{fg}	latent heat of vaporization
Ja	modified Jakob number, $(\rho_f c_{pf} \Delta T_{sub})/(\rho_g h_{fg})$
L	length of heater
m	constant
q	heat flux
q_M	critical heat flux (CHF)
$\tilde{q}_M^*$	dimensionless CHF, $q_M/(\rho_g h_{fg} U)$
$\hat{q}_M$	dimensionless CHF, equation (7)
T	temperature
ΔT_{sat}	wall superheat, $T_w - T_{sat}$
ΔT_{sub}	inlet subcooling, $T_{sat} - T_{in}$
U	mean inlet velocity
We	Weber number, $(\rho_f U^2 L)/\sigma$.

Greek symbols

δ	film thickness
δ_M	thickness of subfilm
δ^*	dimensionless film thickness, δ/L
σ	surface tension
ρ	density
ρ^*	density ratio, ρ_f/ρ_g.

Subscripts

f	liquid
g	vapor
in	inlet
sat	saturation
sub	subcooled
w	wall.

larger than CHF for the smooth surface. Unfortunately, the value of CHF for the GEWA-T surface was not determined. The improved performance of the GEWA-T surface was attributed to an increased surface area and to a large spacing between re-entrant grooves, which prevented the vapor columns from coalescing.

Although boiling in flowing films has been studied [1–4], little has been done to consider the effect of augmented surface structures. Nakayama *et al.* [8] studied evaporation and boiling in a gravity driven R-11 film falling over three enhanced surfaces and a smooth surface. The augmented surfaces consisted of two grooved (microfinned) surfaces, for which the grooves were either aligned (vertical) or perpendicular (horizontal) to the flow direction, and a porous cover plate with subsurface tunnels perpendicular to the flow direction. The heat transfer coefficient for the vertically grooved surface depended on the liquid flow rate, while the coefficient for the porous plate was relatively insensitive to changes in the flow rate. Although the porous plate provided the greatest enhancement, the performance of the vertically grooved surface at its optimum flow rate was comparable to that of the porous plate. Performance of the grooved surfaces was influenced by orientation of the fins relative to the flow direction. While the horizontally grooved surface nucleated first, the vertically grooved surface had superior performance at low heat fluxes. However, in the fully developed nucleate boiling regime, the two boiling curves converged. Although CHF data were not reported for the falling film configuration, such data were reported in a later study involving pool boiling [9]. For pool boiling on a horizontal surface with FC-72 at atmospheric pressure, the microfin surface showed a 90% increase in CHF (based on the planform area) relative to the smooth surface, while the porous plate surface increased CHF by only 6%.

The present study has focused on the enhancement of boiling in a liquid film of FC-72 flowing over a 63.5 mm long, 25.4 mm wide, vertical copper surface. Results for two structured surfaces were compared with those for a smooth surface over film thickness, film velocity and subcooling ranges corresponding to $0.25 < \delta < 1.0$ mm, $0.3 < U < 1.5\,\mathrm{m\,s^{-1}}$, and $0 < \Delta T_{sub} < 16°C$, respectively. A flow deflector, designed to enhance CHF, was also tested with each of the surface geometries. In addition to heat transfer measurements, flow visualization was used to interpret the results.

EXPERIMENTAL SYSTEM

The augmented surfaces considered in this study (Fig. 1) include a microfin surface, which was formed by machining longitudinal grooves in a copper block, and a microstud surface, which was formed by cutting grooves in both the longitudinal and lateral directions. The augmented surfaces have identical groove spacings and depths. The microfin surface was chosen because of the positive results obtained by Nakayama *et al.* [8, 9], when microfins were used for both pool boiling and boiling of a falling film. The microstud surface was chosen to assess the effects of improved lateral wetting [8].

The boiling surfaces were contained within the heater module shown in Fig. 2, which consisted of a low thermal conductivity fiberglass (G-7) substrate, a boron nitride (BN) and chromium wire heat source, and two copper blocks. The heat source was fabricated by cutting a series of shallow grooves in the BN plate adjoining the secondary copper block and winding chromium wire in a serpentine pattern along

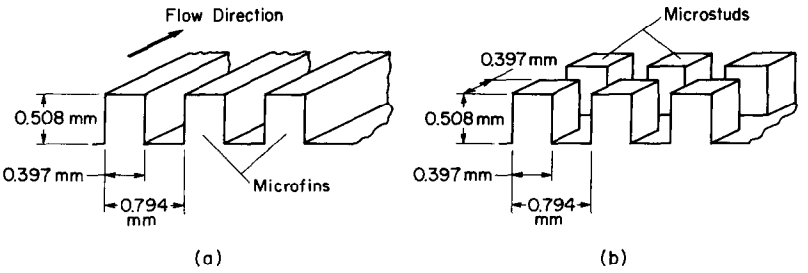

FIG. 1. Augmented surface geometries: (a) microfin, (b) microstud.

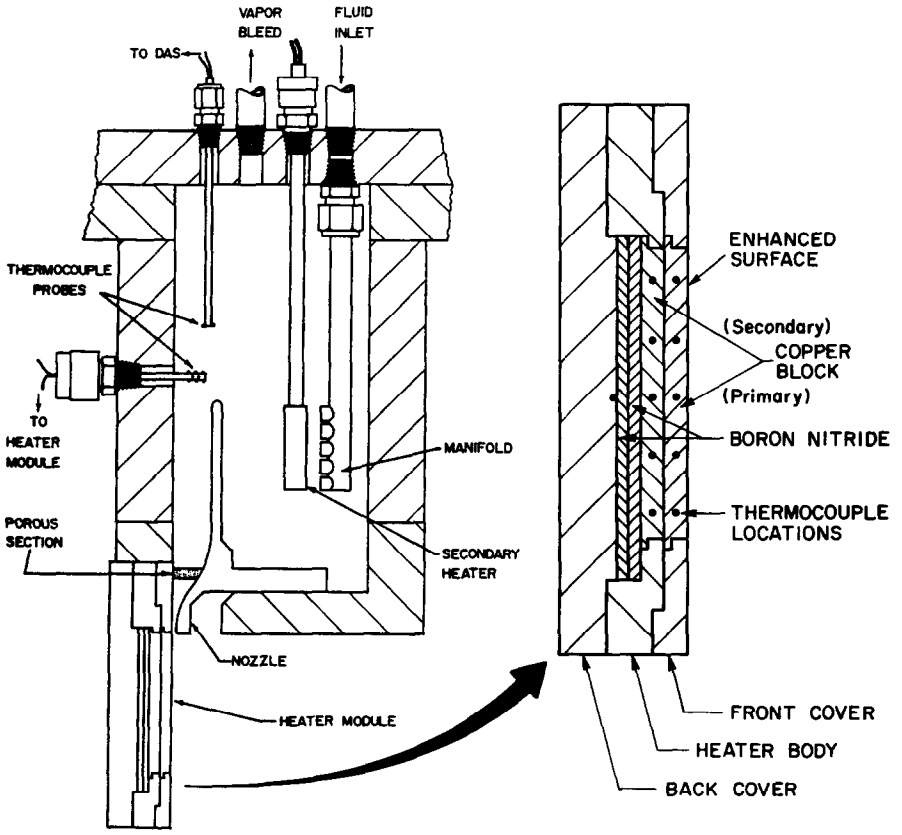

FIG. 2. Schematic of inner test chamber assembly and heater module.

the grooves. The grooves and the interface between the BN plate and the secondary copper block were packed with BN powder to reduce the thermal contact resistance. Two copper blocks were used to allow replacement of the primary block without disturbing the heat source. A thin coating of thermal grease was applied to the interface between the primary (enhanced surface) and secondary copper blocks to reduce thermal contact resistance.

The heater module was mounted on the bottom of an inner test chamber, as shown in Fig. 2. The fluid delivery system (Fig. 3) supplied FC-72 to the inner chamber through a manifold, which directed the liquid to a secondary (cartridge) heater. The heater was used to achieve fine temperature control of the fluid upstream of the nozzle. A copper–constantan thermocouple was used to measure the fluid temperature (T_{in}) at the nozzle inlet, and additional thermocouple probes provided reference junctions for eleven thermocouples located along the centerline of the heater module. A small porous section placed at the mouth of the nozzle provided back pressure to completely fill the inner chamber with fluid, and a bleed port located at the top of the inner chamber allowed trapped vapor to escape into the outer chamber.

The test chamber was an integral part of a high purity, closed-loop fluid delivery system which supplied fluid to the test chamber at a controlled flow rate, temperature, and pressure. The fluid delivery system was also designed to condense vapor generated within the test chamber and to return the condensate

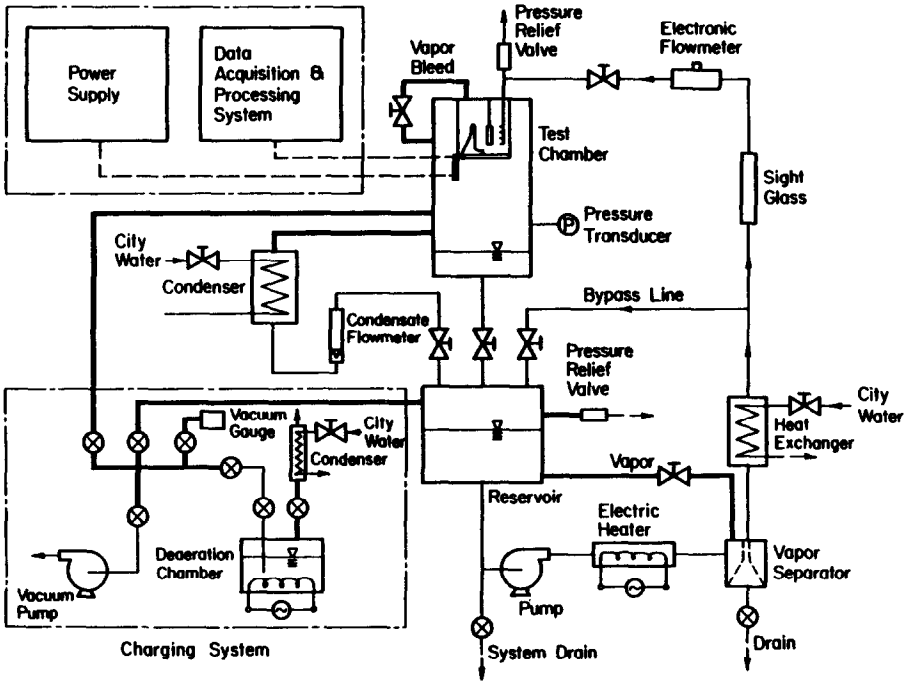

FIG. 3. Schematic of fluid delivery system.

to the system reservoir. As shown in Fig. 3, fluid was drawn from the reservoir by a magnetically coupled stainless steel pump and forced through the primary electric heater, which was regulated by a digital temperature controller, and into a centrifugal phase separator. Vapor generated by the electric heater was separated and routed to the reservoir, while the bulk of the fluid continued to the test chamber. The flow rate, which was controlled by varying the pump speed and the amount of fluid allowed to bypass the test chamber, was measured by an electronic turbine flowmeter. Film velocities were obtained by dividing the volumetric flow rate by the area of the nozzle opening, and film thicknesses were based on the nozzle spacing. Pressure in the test chamber was measured by a strain gage, absolute pressure transducer.

A charging system was used to introduce deaerated fluid to the flow loop. A stainless steel pressure vessel, equipped with four 350 W cartridge heaters and a reflux condenser, was used to deaerate the fluid through vigorous boiling. The fluid was then flashed into the loop, which was initially evacuated to less than 500 μm of Hg.

Experiments were performed for three surface (primary copper block) conditions: (i) a smooth (unaugmented) surface, (ii) the microfin surface, and (iii) the microstud surface. In each case the surfaces were 25.4 mm wide and 63.5 mm long. The surfaces were abraded with 600 grit silicone-carbide sandpaper and cleaned with acetone. To establish the desired operating conditions, the fluid was circulated and heated by the primary electric heater. When the desired temperature, pressure and flow rate were established, power was applied to the heat source.

Boiling curves were generated by manually incrementing the power to the heat source in discrete steps. After each power increment, temperatures throughout the heat source were monitored to determine steady-state conditions in the heater module. Upon reaching steady conditions, which typically took less than 3 min, the power supplied to the heat source, the module temperatures, the system temperatures, the pressure and the flow rate were measured by a Hewlett–Packard 3054 data acquisition system. This procedure was repeated until CHF was detected by a temperature overshoot at the lower edge of the heated surface. A thermocouple in the lower section of the heater module was connected to a protection circuit, which terminated the heater power when a prescribed temperature in the heater was exceeded. The magnitude of the power increment was decreased near CHF to decrease uncertainties associated with its determination.

Heat fluxes reported in the boiling curves are based on the total power supplied to the heat source and the planform area of the boiling surface ($2.54 \times 6.35 = 16.13\,\text{cm}^2$). From a two-dimensional conduction analysis of the heater module, which included experimentally determined contact resistances at the BN–copper and copper–copper interfaces, substrate heat losses were estimated to be less than 2% of the input power. The wall temperature was based on the average of the temperatures measured by thermocouples in the primary copper block. The temperature was corrected for the drop which occurs across the 2.54 mm distance between the thermo-

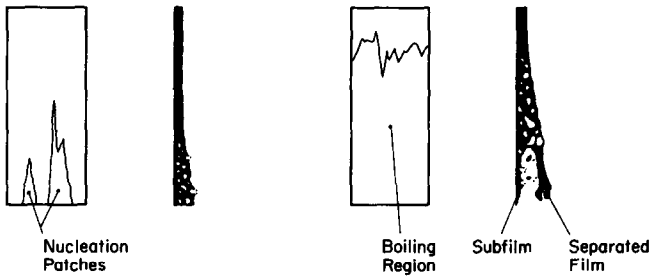

FIG. 4. Representation of boiling development in thin films.

couple locations and the boiling surface. For all heat fluxes other than those close to CHF, only slight temperature variations ($<1°C$) existed between upstream and downstream locations on the copper block, and the block may be considered isothermal. In close proximity to CHF, downstream temperatures in the copper block could exceed the upstream temperature by as much as 3°C.

EFFECTS OF FILM VELOCITY AND THICKNESS

The inception and development of nucleate boiling was similar for each of the three surfaces. In particular, boiling is initiated at preferred nucleation sites near the lower edge of the heated surface. At low heat fluxes, the activation of additional nucleation sites in the wakes of preferred nucleation locations results in the formation of nucleation patches across the span of the lower half of the heater. As represented in Fig. 4(a), the film within the patches is characterized by a longitudinally increasing void fraction. As the heat flux is increased, additional patches develop and spread across the span of the heater and the patch initiation point moves up the heater. At high heat fluxes, the film characteristics resemble those shown in Fig. 4(b), where the patches have coalesced and the boiling initiation point is close to the top of the heater. Near the lower edge of the heater, the void fraction exceeds the value required to maintain a liquid continuum and the film separates, leaving a thin sublayer. This layer, or subfilm, has been reported by other investigators [1–4], and CHF occurs when the subfilm dries out.

Figure 5 shows a comparison of boiling curves for the smooth, microfin and microstud surfaces. As indicated, both augmented surfaces improve heat transfer in the forced convection and nucleate boiling regimes. The inception of boiling occurred over a small range of heat fluxes ($2.0 \times 10^4 \lesssim q \lesssim 3 \times 10^4$ W m^{-2}) for each of the surfaces. Although the microstud surfaces requires the lowest wall superheat for a given heat flux, the microfin surface achieves the highest CHF. Flow characteristics for the microfin surface (Fig. 6) are similar to those described by Mudawwar *et al.* [10] for a smooth surface, although the film separation

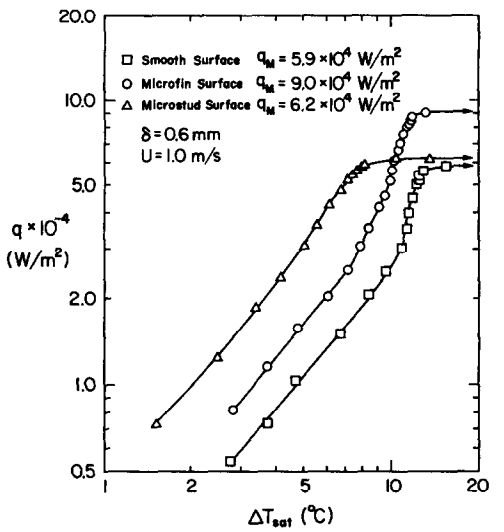

FIG. 5. Effect of surface geometry on boiling performance.

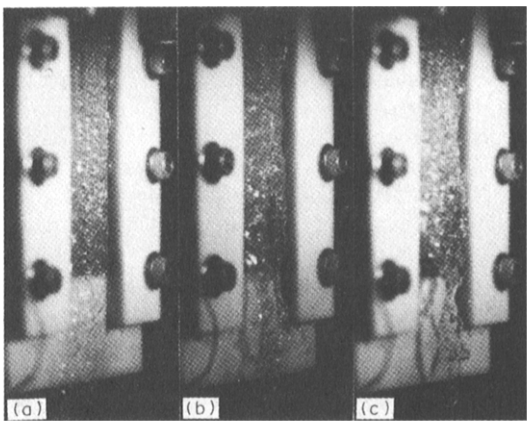

FIG. 6. Film characteristics on the microfin surface for increasing flux ($U = 0.5$ m s^{-1}, $\delta = 0.66$ mm): (a) $0.35q_M$, (b) $0.95q_M$ and (c) q_M.

and subfilm dryout phenomena occur at larger heat fluxes. The approximately 50% enhancement in CHF may be due to one or both of two factors. The longitudinal grooves may allow surface tension forces to more effectively maintain contact between the fluid

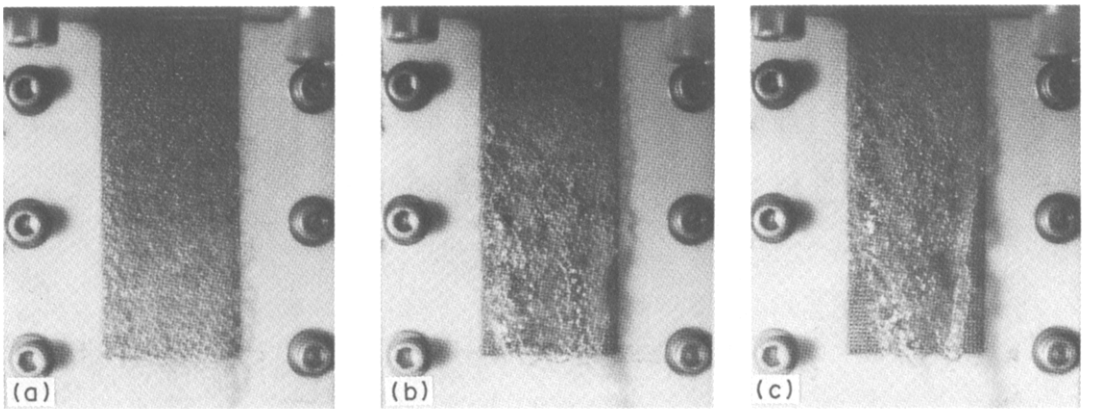

FIG. 7. Film characteristics on the microstud surface for increasing heat flux ($U = 1.5\,\mathrm{m\,s^{-1}}$, $\delta = 0.25\,\mathrm{mm}$): (a) $0.60q_M$, (b) $0.90q_M$ and (c) q_M.

and the surface, and/or they may prevent subfilm dryout by constraining the lateral spread of dry patches. For the microstud surface, CHF is approximately the same as that for the smooth surface. The relatively small slope in the boiling curve and the small CHF for the microstud surface may be attributed to disruption and fragmentation of the film by the studs. As shown in Fig. 7, flow over the microstud surface is characterized by a large number of small bubbles. Film break-up advances film separation and the onset of CHF. The slight convergence of the film towards the middle portion of the heated surface in Fig. 7(b) shows that, at 90% of CHF, significant separation has occurred. For this condition, there are areas which are intermittently cooled by reattachment of the separated film.

An important feature of Fig. 5 concerns the absence of a temperature overshoot at the inception of boiling. Murphy and Bergles [11] have found that a porous surface eliminates hysteresis in forced convective boiling. However, Bergles and Chyu [6] and Marto and Lepere [7] found a large temperature overshoot when a porous surface is used in pool boiling. The fact that the porous surface failed to prevent hysteresis in pool boiling was explained by Bergles and Chyu [6] in terms of a required disturbance level. They stated that the level of disturbance present in a forced convective flow was large enough to eliminate hysteresis.

Slopes m for the proportionality $q \propto \Delta T_{\mathrm{sat}}^{m}$ in the fully developed nucleate boiling regime of flowing liquid films have been reported to vary from $m = 1.4$ [1] to 1.8 [12]. However, average slopes for this study were $m = 2.5$, 2.0 and 1.3 for the smooth, microfin and microstud surfaces, respectively.

The effect of film velocity on the smooth surface boiling curve (Fig. 8) is consistent with the results of Toda and Uchida [1] and Baines *et al.* [3]. The effect of velocity is pronounced in the forced convection region and for CHF, but the curves collapse in the fully developed nucleate boiling regime. Figures 8–10 show that CHF increases with increasing velocity for

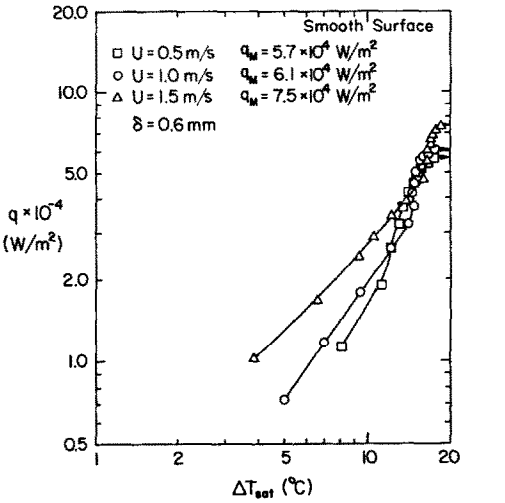

FIG. 8. Effect of film velocity on smooth surface boiling curve.

each of the surfaces of this study. However, the effect of velocity is more pronounced for the augmented surfaces than for the smooth surface. Figure 9 shows that velocity influences the entire boiling curve for the microfin surface, with the curves for larger velocities shifted slightly to the left. For the microstud surface (Fig. 10), fluid motion is influenced as much by the studs as it is by vapor production and the effect of velocity is pronounced.

Figure 11 shows that film thickness had only a slight effect on the boiling curve for the microfin surface. Differences between the results for $\delta = 0.25\,\mathrm{mm}$ and those for film thicknesses of 0.6 and 1.0 mm are likely to be due to incomplete wetting of the fins when δ is less than the fin height (0.508 mm). The crossover in the curve for the 0.25 mm film thickness and those for the other film thicknesses at $q \approx 4 \times 10^4\ \mathrm{W\,m^{-2}}$ may result from a thickening of the film due to increased void fraction, which provides greater wetting of the fins. A slight increase in CHF was also associated with

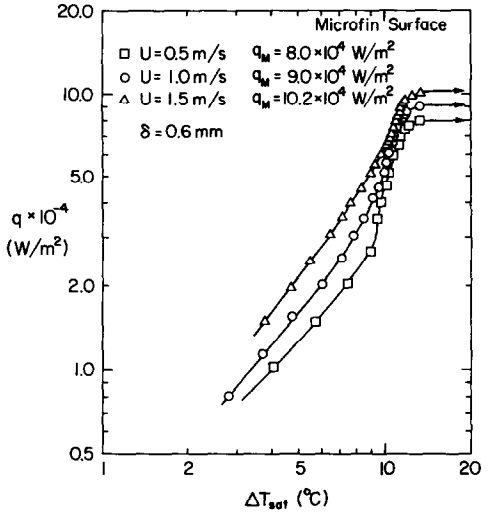

FIG. 9. Effect of film velocity on microfin surface boiling curve.

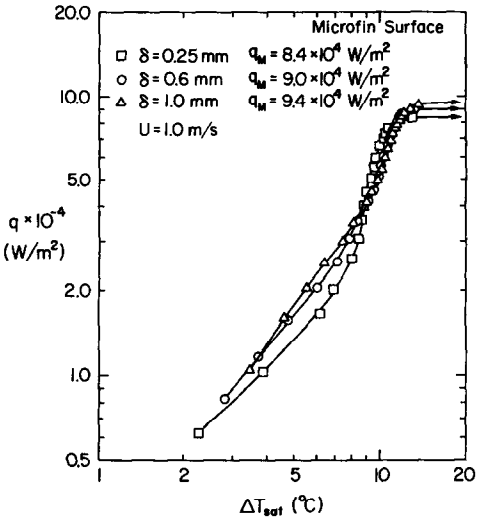

FIG. 11. Effect of film thickness on microfin surface boiling curve.

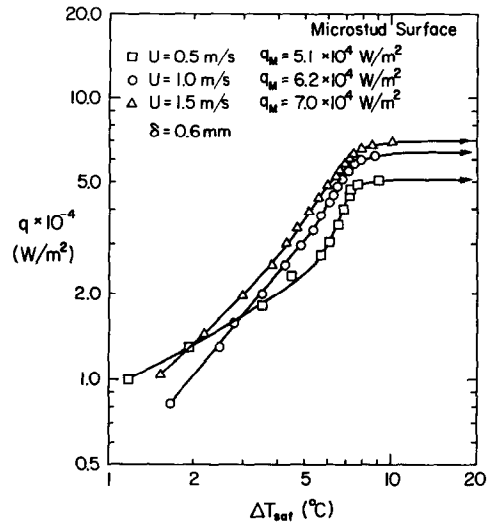

FIG. 10. Effect of film velocity on microstud surface boiling curve.

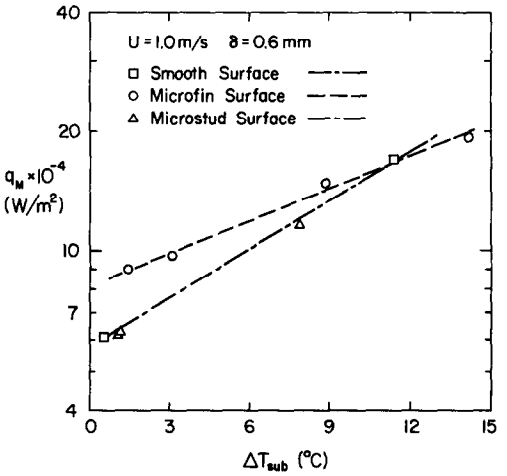

FIG. 12. Effect of subcooling on CHF.

increasing film thickness for each of the three surfaces.

Figure 12 shows that subcooling significantly enhances CHF and that the effect is more pronounced for the smooth and microstud surfaces than for the microfin surface. In addition, there is an exponential dependence of CHF on subcooling for the subcooling range of this study, while for pool boiling CHF increases linearly with subcooling [13]. The microbubbles which were observed to form in the subcooled film enhanced heat transfer but did not significantly increase the downstream void fraction, since bubble growth was retarded by the subcooled liquid.

CORRELATION OF THE CHF DATA

As previously described, CHF results from two phenomena, which include film breakdown and separation from the surface and subsequent dryout of the subfilm which is left on the surface. Previous studies [2, 3, 10, 14] have established the following primary dimensionless groups to correlate the corresponding CHF values:

$$\tilde{q}_M^* \equiv \frac{q_M}{\rho_g h_{fg} U}, \quad We \equiv \frac{\rho_f U^2 L}{\sigma}, \quad \rho^* \equiv \frac{\rho_f}{\rho_g}. \tag{2}$$

Although additional dimensionless groups, such as the Reynolds and Froude numbers, have also been suggested to account for viscous and buoyancy forces, respectively, their influence on CHF is typically neglected. Therefore, the following correlation has been proposed

$$\tilde{q}_M^* \equiv C_1 \rho^{*C_2} (1/We)^{C_3}. \tag{3}$$

In this study, two parameters not included in equation (3) were observed to influence CHF. Hence, to include the effects of film thickness (δ) and subcooling

Table 1. CHF correlation coefficients

	C_1	C_3	C_4	C_5	$\bar{e}$	e_{max}
Smooth	0.0941	0.400	0.213	0.0570	5.6	16
Microfin	0.102	0.428	0.0958	0.0387	3.4	8
Microstud	0.0686	0.385	0.183	0.0564	3.7	12

(ΔT_{sub}), the following dimensionless groups may be introduced:

$$\delta^* \equiv \frac{\delta}{L}, \quad Ja \equiv \frac{c_{pf}\Delta T_{sub}}{\rho_g h_{fg}} \tag{4}$$

where the length scale used to nondimensionalize the film thickness is taken as the length of the heater. The energy associated with liquid subcooling is included in a modified Jakob number, which is a ratio of the sensible to latent heat. Hence, the correlation considered for this study is of the form

$$\bar{q}_M^* = C_1 \rho^{*C_2} (1/We)^{C_3} \delta^{*C_4} \exp(C_5 Ja). \tag{5}$$

Although the density ratio is a strong function of pressure, data of this study correspond only to atmospheric conditions. Hence, the exponent on ρ^* was fixed at $C_2 = 0.867$, which is the result obtained by Katto and Ishii [2] for a wall jet. The exponential dependence of CHF on the Jakob number was observed to best correlate the effect of subcooling.

The results of applying least-squares curve fits to the CHF data of this study are summarized in Table 1, which includes the average absolute and maximum percent errors in the correlation, as well as the correlation coefficients. The parameter ranges used in developing the correlation correspond to $0.25 < \delta < 1.0$ mm, $0.3 < U < 1.5\,\mathrm{m\,s^{-1}}$, $0 < \Delta T_{sub} < 16$°C, and $L = 63.5$ mm. The correlation is contrasted with the data in Fig. 13, where $\hat{q}_M$ is defined as

$$\hat{q}_M = \frac{\bar{q}_M^*}{C_1 \rho^{*0.867} \delta^{*C_3} \exp(C_4 Ja)}. \tag{6}$$

The nearly equivalent Weber number dependence for each of the surfaces is surprising, since the surface geometry should influence the effects of velocity and surface tension. The dependence of q_M on $U^{(1-2C_3)}$ indicates that the microfin surface, which has the largest inverse Weber number dependence, actually has the smallest velocity dependence. This result may be due to the fact that sublayer dryout occurred between the fins, where the flow was influenced more by the geometry than by separation of the film. The fact that the velocity dependence of q_M is largest for the microstud surface suggests that the sensitivity of flow separation to velocity is amplified by the studs.

Mudawwar *et al.* [10] recently presented a hydrodynamic model of CHF in flowing liquid films, for which film breakdown was presumed to be caused by a Helmholtz instability that occurs in vapor jets supplying the bubbles. When the instability occurs, a thin liquid layer, the thickness δ_M of which is of the order of the critical Helmholtz wavelength, remains

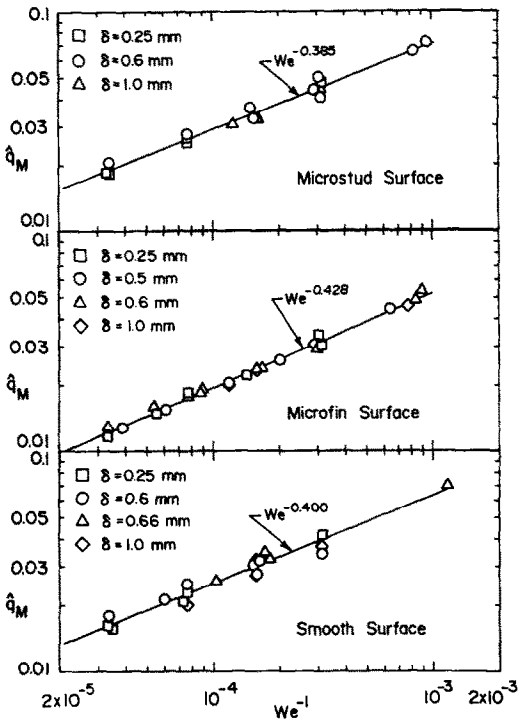

FIG. 13. Comparison of CHF data with correlations.

on the heated surface. The expression for the Helmholtz wavelength at typical operating pressures was simplified to give the following equation for the sublayer thickness

$$\delta_M \propto \frac{\sigma}{\rho_g \left[\frac{q}{\rho_f h_{fg}}\right]^2} \tag{7}$$

where $q/(\rho_f h_{fg})$ is the average velocity of vapor perpendicular to the heated surface. For saturated films, CHF was postulated to occur when the latent heat of the liquid subfilm is balanced by the heat rate at the boiling surface

$$q_M L = \rho_f U \delta_M h_{fg}. \tag{8}$$

When equations (7) and (8) are combined for saturated films, they yield an expression of the form given by equation (3) with $C_2 = 2/3$ and $C_3 = 1/3$. The model also predicts the following ratio of CHF at subcooled conditions to CHF at saturated conditions

$$\frac{q_{M,sub}}{q_{M,sat}} = \left[1 + \frac{c_{pf}\Delta T_{sub}}{h_{fg}}\right]^{1/3} \times \left[1 + C_{sub}\frac{\rho_f c_{pf}\Delta T_{sub}}{\rho_g h_{fg}}\right]^{2/3}. \tag{9}$$

The value of $C_{sub} = 0.16$ which was recommended [10] provides reasonable agreement, for low subcooling, with the exponential dependence observed for the smooth surface and the subcooling range of this study.

Although film thickness, which was observed to

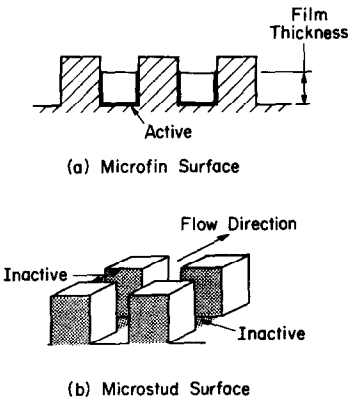

FIG. 14. Active and inactive microlayer evaporation areas for (a) microfin surface and (b) microstud surface.

have a slight effect on CHF in this study, was not included in the foregoing model, the mechanism proposed by Mudawwar *et al.* [10] offers a possible explanation for the effects of the augmented surfaces on CHF. Near the upstream edge of the heated surface, the film thickness may be assumed to be equal to the nozzle spacing. For the microfin surface, nozzle settings less than the fin height therefore provide an active area for microlayer evaporation which includes the region between the fins and that portion of the fin sides up to the height of the film (Fig. 14(a)). Hence, there should be an increase in CHF as the film thickness increases due to an increase in the area available for microlayer evaporation. When the film thickness exceeds the fin height, the fin tip would also become active, further increasing CHF. The film thickness also influences the actual film velocity for a given average velocity based on the nozzle opening. The fins provide a blockage which reduces the effective flow area and hence increases the velocity. As the film thickness is increased, however, the fins provide less blockage and the actual velocity approaches the average velocity. Hence, there is likely to be a critical film thickness, beyond which there is little improvement in CHF.

For the microstud surface, film breakup may leave essentially inactive regions on surfaces with normals parallel to the flow direction and in base regions between such surfaces (Fig. 14(b)). There may then be little increase in active surface area relative to the smooth surface and hence little increase in CHF. The argument used to explain the effect of film thickness for the microfin surface may also be applied to the microstud surface.

EFFECT OF A FILM DEFLECTOR

Because film separation occurs prior to CHF, there exists the possibility of extending CHF by redirecting the separated portion of the film back to the heated surface. A louvered flow deflector designed to extend CHF without pressurizing the liquid film was fabri-

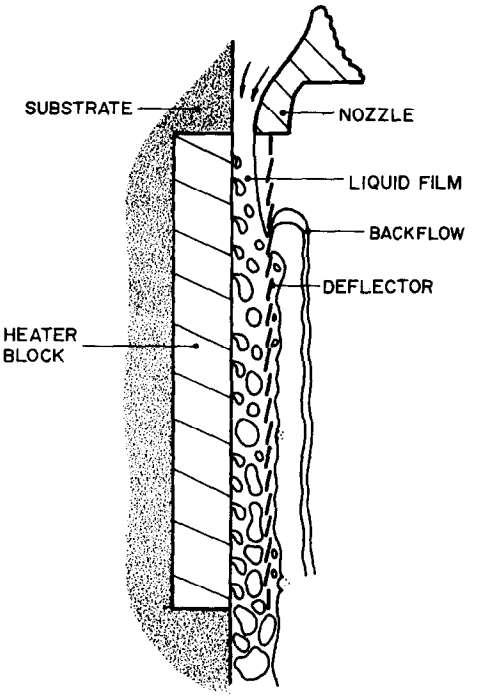

FIG. 15. Film characteristics at high heat fluxes with deflector.

cated from 0.152 mm thick brass sheet stock in which louvers were formed by bending 18 webs, made by cutting 0.794 mm wide slots spaced on 3.175 mm centers, approximately 12°. The deflector was mounted 2.54 mm from the base of the boiling surface and was held in contact with the edge of the surface (Fig. 15).

Several observations could be made concerning the effect of the deflector on the flow. Because the deflector was mounted 2.54 mm from the base of the boiling surface and the film thickness was $\delta = 0.6$ mm for all the deflector runs, there was no initial contact between the film and the deflector. When nucleation occurred and the film thickened due to the increased void fraction, contact with the deflector occurred and bubbles were observed to erupt through the gaps between the louvers. As the heat flux was increased, the liquid contact point moved upstream, and an increasing fraction of the film began to flow outside the louvers. The fluid on the outside of the louvers was observed to have an upward velocity component as it emerged from the louvers. When the contact point approached the top of the heater, the backflow between the louvers became strong enough to force a liquid stream to be projected away from the heater, as shown in Fig. 15. The presence of the backflow indicates that some pressurization occurred between the louvered deflector and the boiling surface.

Figure 16 compares the performance of each surface with and without the deflector. The most significant result is the increase in CHF provided by the deflector. For the augmented surfaces, the curves corresponding to use of the deflector are shifted slightly to the left, and at large heat fluxes there is

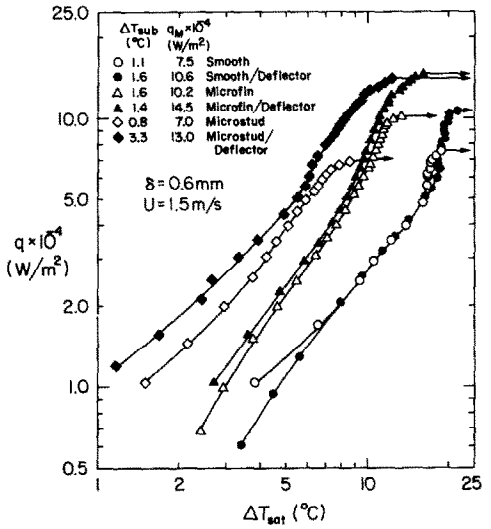

FIG. 16. Effect of deflector on boiling performance.

Table 2. Percent increase in CHF with deflector

U (m s^{-1})	Smooth	Microfin	Microstud
0.5	—	30	71
1.0	16	44	74
1.5	41	42	86

a decrease in the slope. The change in slope occurs approximately at the flux corresponding to CHF for the undeflected film and is believed to be associated with film breakdown and a transition from heat transfer by nucleate boiling to droplet cooling by the deflected liquid. Table 2 shows that, irrespective of the film velocity, the effect of the deflector is greatest for the microstud surface and that, for each surface, the effectiveness increases with increasing velocity. With increasing velocity, the deflector is able to redirect more of the separated film to the surface.

Table 2 also shows that the improvements in CHF associated with the enhanced surfaces were larger than those for the smooth surface. This result is, in part, due to the fact that the height of the surface structures reduced the effective deflector height from 2.54 mm for the smooth surface to slightly over 2 mm for the enhanced surfaces. The foregoing observation suggests that an optimum deflector height may exist. As the deflector is brought closer to the heated surface, increases in CHF may be limited by a transition in the mode of CHF from film separation to flooding.

The maximum improvement in CHF occurred for the microstud surface. Because the microstuds break up the film, contact with the deflector occurs at a smaller heat flux than for the other surfaces. However, backflow over the louvers is delayed because the studs provide smaller liquid droplets.

SUMMARY

Experiments have been performed to determine the extent to which boiling heat transfer in a falling liquid film may be enhanced by using structured surfaces and/or a flow deflector. Key results are given below.

(1) For flow of a falling film over plain, microfin and microstud surfaces, boiling begins with the activation of nucleation sites at the trailing edge of the surface. With increasing heat flux, the onset of nucleation moves up the heater and more sites become activated in the lateral (crossflow) direction. The void fraction increases in the flow direction until film breakdown and separation occurs at the trailing edge, leaving a thin subfilm. The onset of CHF corresponds to dry patch formation in the subfilm. By allowing surface tension forces to more effectively maintain contact between the fluid and the surface and inhibiting the lateral spread of dry patches, the longitudinal grooves in the microfin surface delay the onset of CHF. In contrast the intermittent studs in the microstud surface act to break-up the film, thereby advancing film separation and the onset of CHF.

(2) The microfin surface enhances nucleate boiling and CHF relative to a plain surface. However, although the microstud surface provides superior performance in the nucleate boiling regime, it does not enhance CHF relative to a smooth surface.

(3) For each surface, CHF increases with increasing film velocity, thickness and subcooling. The effects are correlated in terms of the Weber number, a dimensionless film thickness and a modified Jakob number.

(4) Significant CHF enhancement is achieved by installing a louvered deflector over the falling film. The enhancement increases with increasing velocity and is largest for the microstud surface.

Acknowledgement—Support for this research by the IBM Corporation is gratefully acknowledged.

REFERENCES

1. S. Toda and H. Uchida, Study of liquid film cooling with evaporation and boiling, *Trans. JSME* **38**, 1830–1838 (1972).
2. Y. Katto and K. Ishii, Burnout in a high heat flux boiling system with a forced supply of liquid through a plane jet, *Proc. of Sixth International Heat Transfer Conference*, Vol. 1, pp. 435–440 (1978).
3. R. P. Baines, M. A. El-Masri and W. M. Rohsenow, Critical heat flux in flowing liquid films, *Int. J. Heat Mass Transfer* **27**, 1623–1629 (1984).
4. I. Mudawwar, M. A. El-Masri, C. Wu and J. Ausman-Mudawwar, Boiling heat transfer and critical heat flux in high-speed rotating liquid films, *Int. J. Heat Mass Transfer* **28**, 795–806 (1985).
5. R. L. Webb, The evolution of enhanced surface geometries for nucleate boiling, *Heat Transfer Engng* **2**, 46–69 (1981).
6. A. E. Bergles and M. C. Chyu, Characteristics of nucleate pool boiling from porous metallic coatings, *J. Heat Transfer* **104**, 279–285 (1982).
7. P. J. Marto and V. J. Lepere, Pool boiling heat transfer from enhanced surfaces to dielectric fluids, *J. Heat Transfer* **104**, 292–299 (1982).
8. W. Nakayama, T. Daikoku and T. Nakajima, Enhancement of boiling and evaporation on structured surfaces with gravity driven film flow of R-11, *Heat Transfer*

1982, pp. 409–414. Hemisphere, Washington, D.C. (1982).
9. W. Nakayama, T. Nakajima and S. Hirasawa, Heat sink studs having enhanced boiling for cooling of microelectronic components, ASME Paper No. 84-WA/HT-89 (1984).
10. I. A. Mudawwar, T. A. Incropera and F. P. Incropera, Boiling heat transfer and critical heat flux in liquid films falling on vertically-mounted heat sources, *Int. J. Heat Mass Transfer* **30,** 2083–2095 (1987).
11. R. W. Murphy and A. E. Bergles, Subcooled flow boiling of fluorocarbons—hysteresis and dissolved gas effects on heat transfer, *Proc. of 1972 Heat Transfer and Fluid Mechanics Institute*, pp. 400–416. Stanford University Press, Stanford, California (1972).
12. O. Parizhskiy, V. Chepurnenko, L. Lagota and L. Taranets, Study of boiling heat transfer with a falling film of refrigerant, *Heat Transfer—Soviet Res.* **4,** 43–47 (1972).
13. H. J. Ivey and D. J. Morris, On the relevance of the vapor–liquid exchange mechanism for subcooled boiling heat transfer at high pressure, U.K. Rept. UEEWR-137, Winfrith (1962).
14. M. Monde and Y. Katto, Burnout in a high-flux boiling system with an impinging jet, *Int. J. Heat Mass Transfer* **21,** 295–305 (1976).

ACCROISSEMENT DE CHF DANS DES FILMS TOMBANTS LIQUIDES DE FLUOROCARBURE SUR DES SURFACES STRUCTUREES ET DES DEFLECTEURS D'ECOULEMENT

Résumé—Des expériences d'ébullition sont faites avec un film liquide de fluorocarbone (FC 72) tombant sur une surface chaude verticale. Une ébullition intense sépare la plupart du film de la surface, laissant une mince pellicule, et le CHF est associé à l'assèchement de cette pellicule. Des surfaces avec augmentation de microailettes accroît le CHF par rapport aux surfaces lisses. Une plaque ajourée montée parallèlement à la surface chaude augmente aussi le CHF en défléchissant vers l'arrière le liquide séparé sur la surface chaude, ce qui retarde l'assèchement de la pellicule liquide.

ERHÖHUNG DER KRITISCHEN WÄRMESTROMDICHTE (CHF) BEI STRÖMENDEN FLÜSSIGKEITSFILMEN AUS FLUORKOHLENWASSERSTOFFEN UNTER VERWENDUNG VON STRUKTURIERTEN OBERFLÄCHEN UND STRÖMUNGSDEFLEKTOREN

Zusammenfassung—Es wurden Experimente zum Sieden von Fluorkohlenwasserstoff FC-72 in einem Flüssigkeitsfilm ausgeführt, der über eine senkrechte, beheizte Oberfläche fällt. Durch heftiges Sieden wird der größte Teil des Filmes von der Oberfläche abgetrennt. Zurück bleibt ein dünner Unterfilm. CHF wird durch ein Austrocknen des Unterfilms gekennzeichnet. An Oberflächen, welche durch Mikrorippen vergrößert sind, liegt CHF höher als bei glatten oder mikrostrukturierten Oberflächen. Eine zusätzliche, parallel zur beheizten Oberfläche montierte Platte erhöht CHF ebenfalls, und zwar dadurch, daß die abgetrennte Flüssigkeit zur beheizten Oberfläche zurückgelenkt wird, was das Austrocknen des Unterfilms verzögert.

УВЕЛИЧЕНИЕ КРИТИЧЕСКОГО ТЕПЛОВОГО ПОТОКА ПРИ ТЕЧЕНИИ ЖИДКИХ ПЛЕНОК ФТОРУГЛЕРОДА ЗА СЧЕТ ИСПОЛЬЗОВАНИЯ СТРУКТУРИРОВАННЫХ ПОВЕРХНОСТЕЙ И ДЕФЛЕКТОРОВ ПОТОКА

Аннотация—Проведены эксперименты по кипению фторуглерода (ФУ-72), стекающего в виде пленки по вертикальной нагреваемой поверхности. При развитом кипении большая часть пленки отделялась от поверхности нагрева, оставляя на ней тонкий подслой, с высыханием которого связано наступление критического теплового потока (КТП). На поверхностях с микроребристой шероховатостью отмечался более высокий КТП, чем на гладких или на поверхностях с микроигольчатой шероховатостью. Использование пластины с жалюзями, помещенной параллельно поверхности нагрева, также приводило к увеличению КТП, так как жалюзи возвращали отделившуюся пленку к поверхности нагрева, и высыхание ее тонкого подслоя на поверхности затягивалось.